Optical homodyne receiver utilizing image rejection in FSK/ASK re-modulation WDM-PON

Yuan Fang (方 圆), Xiao Liu (刘 霄), Xi Zheng (郑 曦), Chunning Hou (侯春宁), Wuliang Fang (方武良), Bo Huang (黄 博), Xinying Li (李欣颖), Shumin Zou (邹书敏), Junwen Zhang (张俊文), Yufeng Shao (邵宇丰), and Nan Chi (迟 楠)*

Department of Communication Science & Engineering, State Key Laboratory of ASIC & System, Fudan University, Shanghai 200433, China

**E-mail: nanchi@fudan.edu.cn*

Received June 9, 2010

Optical frequency shift keying (FSK) homodyne detection utilizing image rejection in FSK/amplitude shift keying (ASK) re-modulation wavelength-division-multiplexed passive optical network (WDM-PON) is proposed and demonstrated. Image rejection is adopted to achieve better performance. We show the result in back-to-back and 40-km distance respectively and apparent improvement is obtained in the latter situation by using image rejection. Several factors which affect the image rejection receiver are analyzed in order to find out the optimum parameters. Result shows that the presented scheme is suitable for super long reach access network, especially for future metro access network.

OCIS codes: 060.2330, 060.2360.

doi: 10.3788/COL20100809.0906.

Wavelength-division-multiplexed passive optical network (WDM-PON) is a promising technology for future broadband access network because of its high capacity, large coverage range, and cost-effective configuration[1]. Recently the re-modulation scheme has been proposed to achieve high speed centralized light source (CLS) WDM-PON. By utilizing orthogonal modulation technology, several re-modulation schemes have been deployed in access network[2−6]. Frequency shift keying (FSK) modulation format enables differential detection scheme and simulations have shown that it has good gain of optical signal-to-noise ratio (OSNR) sensitivity in 10-Gb/s transmission systems[7], thus it has aroused increasing attention. Several different methods to generate FSK signal have been introduced and an orthogonal FSK/amplitude shift keying (ASK) re-modulation scheme in WDM-PON has been simulated and analyzed[8−10]. However, FSK demodulation in PON needs improving urgently. In this letter, we propose optical FSK homodyne detection utilizing image rejection in FSK/ASK re-modulation WDM-PON. It is simple and cost-effective since it does not require an external modulator, thus allowing higher launch power and a more compact transmitter[11−13]. Image rejection receiver (IRR) can provide better sensitivity and allow extremely narrow channel interval. We compare image rejection detection with just using band-pass filter. Simulation results show that the bit error rate (BER) is significantly improved, especially in long reach. Meanwhile, several factors which may affect the image rejection detection are analyzed. We vary the values of three factors including delay time, phase shift, and couple factor to optimize the system performance. IRR for a 40-Gb/s retum-to-zero (RZ)-FSK downstream is proposed and its advantage in super long reach access network is demonstrated.

Optical image rejection is attractive since it reduces crosstalk caused by image band signals and enables extremely narrow channel spacing. Figure 1 shows the configuration of IRR and its operation. The IRR consists of an optical 90° hybrid, two dual-detector balanced optical receivers (DBORs), and an electrical 90° hybrid. The operation of the IRR is as follows. The local laser and the signal lights are combined in optical hybrid which contains 3-dB optical coupler and polarizing beam splitter (PBS). Between the signal and local light, one is to be linearly polarized while the other is circularly polarized. The light intensity is divided equally between the two branches. Detected intermediate frequency (IF) signals have in-phase (I) and quadrature-phase (Q) respectively, expressed as

$$\mathrm{I} = H_{\mathrm{i}}(f)\cos(2\pi f t), \tag{1}$$

$$\mathrm{Q} = H_{\mathrm{q}}(f)\cos(2\pi f t + 2\pi f\tau + \Delta\theta), \tag{2}$$

where f is the IF with positive value, τ is the delay time between I branch and Q branch, $\Delta\theta$ is the phase difference between I/Q signals, $H_{\mathrm{i}}(f)$ and $H_{\mathrm{q}}(f)$ are the gain functions of DBOR. These IF signals are combined in the electrical hybrid which contains multiplier and differentiator. The output can only be obtained at one port of electrical hybrid. The outputs of the electrical hybrid are given as

$$\begin{aligned} U_{\mathrm{r}} = \big[&H_{\mathrm{i}}(f)\cos(2\pi f t) + H_{\mathrm{q}}(f) \\ &\cdot\cos\big(2\pi f t + 2\pi f\tau + \Delta\theta - \frac{\pi}{2}\big)\big]/\sqrt{2}, \end{aligned} \tag{3}$$

$$\begin{aligned} U_{\mathrm{i}} = \big[&H_{\mathrm{i}}(f)\cos\big(2\pi f t - \frac{\pi}{2}\big) + H_{\mathrm{q}}(f) \\ &\cdot\cos(2\pi f t + 2\pi f\tau + \Delta\theta)\big]/\sqrt{2}, \end{aligned} \tag{4}$$

where U_{r} is the real output and U_{i} is the image output. The image rejection suppression is defined by power ratio between U_{i} and U_{r}, given as

$$\begin{aligned} \xi'[\mathrm{dB}] &= -10\lg\xi(f) \\ &= -10\lg\frac{1+S^2-2S\sin(2\pi f\tau+\Delta\theta)}{1+S^2+2S\sin(2\pi f\tau+\Delta\theta)}, \end{aligned} \tag{5}$$

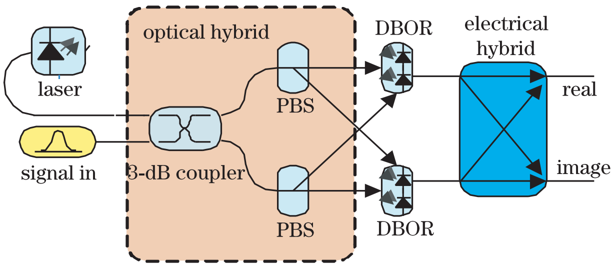

Fig. 1. Principle of IRR.

where S is the gain difference between the branches and $S^2=[H_q(f)/H_i(f)]^2$.

In the scheme, the downstream data are carried by a 40-Gb/s FSK signal and the upstream signal is 2.5-Gb/s ASK signal re-modulated directly on the downstream signal. The upstream and downstream are transmitted in full duplex. As shown in Fig. 2, in the optical line terminal (OLT), two continuous-wave (CW) lights with carefully selected frequencies in 193.0 and 193.1 THz are utilized as the FSK source. The signal

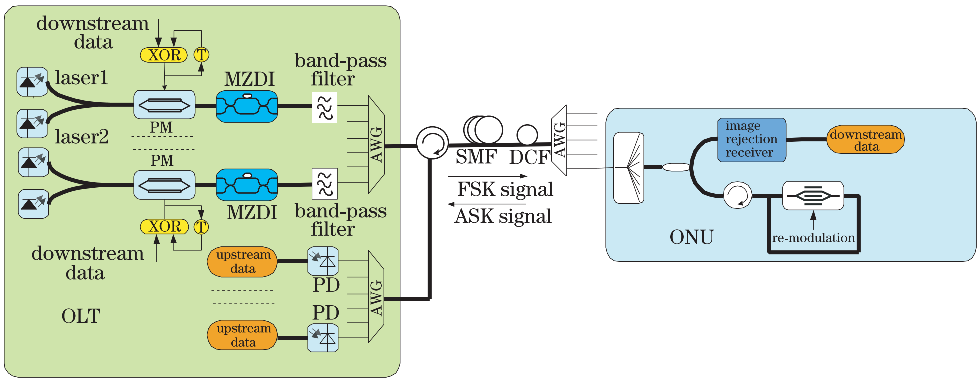

Fig. 2. Schematic for orthogonal FSK/ASK re-modulation in WDM-PON using image rejection. PD: photodetector; SMF: single-mode fiber; DCF: dispersion compensating fiber.

is input to a phase modulator (PM) to undergo DPSK modulation, and then sent to Mach-Zehnder delay interferometer (MZDI). The carefully selected center frequencies of two beams enable one beam to be at the maximum transmission of the MZDI (constructive interference) while the other to be at the minimum transmission (destructive interference). In this way, the data streams of two wavelengths are logically inverted but identical, and a RZ-FSK signal with optical pulse in every bit slot is generated. In the optical network unit (ONU), IRR is used, of which the principle has been explained. Meanwhile, the 2.5-Gb/s upstream data are modulated onto the received downstream signal to achieve an orthogonal FSK/ASK re-modulation. By using the arrayed waveguide grating (AWG) which can perform wavelength multiplexer/de-multiplexer functions as remote node (RN), the system can be extended to WDM architecture.

The optical spectra for FSK and ASK signals are shown in Fig. 3. Since ASK signal is directly modulated on FSK signal, the upstream waveform is influenced by the downstream. The upstream received in OLT will not be ideal.

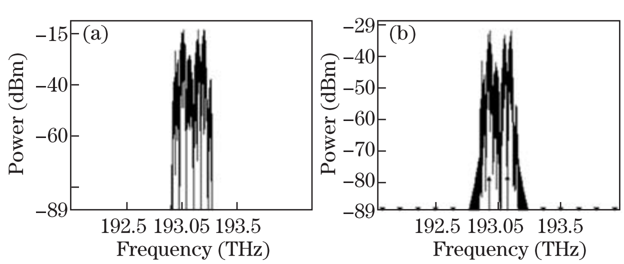

Fig. 3. Measured optical spectra for (a) 40-Gb/s FSK signal and (b) 2.5-Gb/s ASK signal.

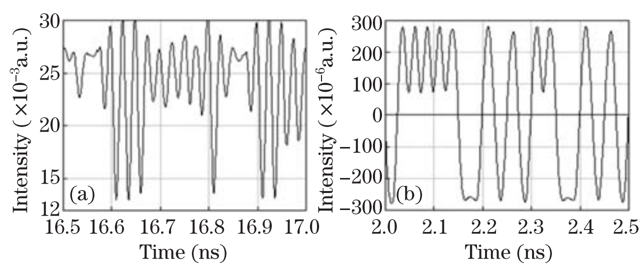

Fig. 4. Measured waveforms for (a) band-pass filter and (b) image rejection.

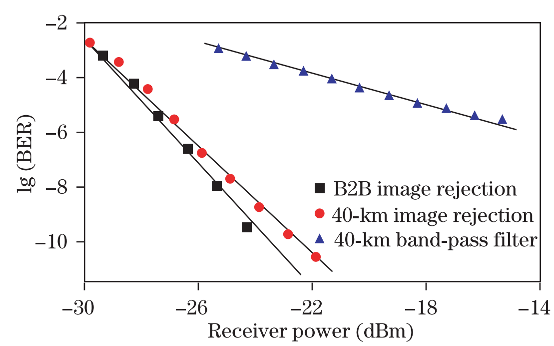

Fig. 5. Measured BER curves versus received downstream power. B2B: back-to-back.

The electrical waveforms for filter direct detection and image rejection detection on 20 km are shown in Fig. 4. More ideal waveform is obtained for image rejection.

We investigate the BER performance by varying the received power before the prepositive amplifier of the receiver in the situation of back-to-back and 40-km single-mode fiber (SMF), as shown in Fig. 5. We investigate

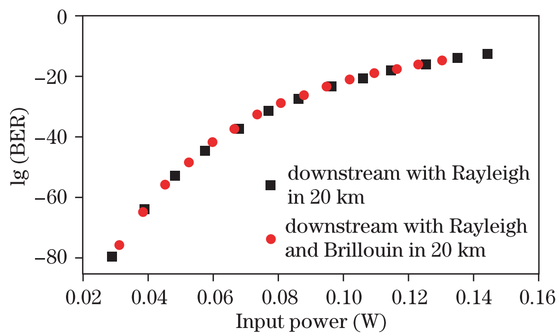

Fig. 6. Measured BER curves versus input power.

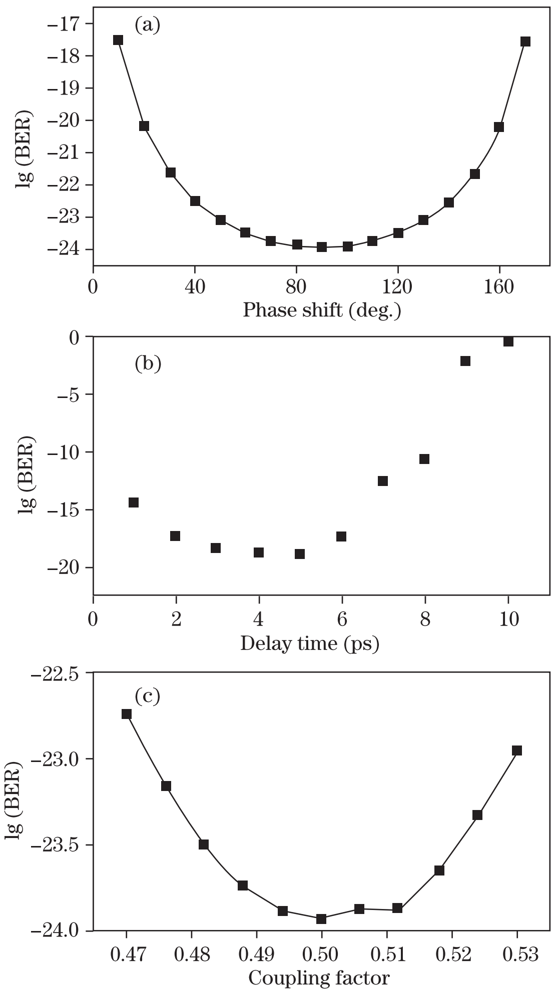

Fig. 7. Measured sensitivity curves versus (a) phase shift, (b) delay time, and (c) coupling factor.

both filter and image rejection situation. As expected, apparent enhancement is obtained when image rejection is applied. In 40-km distance, image rejection still guarantee pretty good performance while BER performance becomes terrible if we just use band-pass filter.

Downstream bit rate as a function of input power in 20 km is shown in Fig. 6. The best input power is between 21.5 and 22 dBm when only Rayleigh scattering is considered. Result is similar when both Rayleigh scattering and Brillouin scattering are taken into account.

The tolerance to delay, phase shift, and coupler imbalance of image rejetion receiver are shown in Figs. 7 (a)–(c), respectively. We take coupler imbalance into consideration and search for the best delay time and phase shift as well. Figure 7(a) shows sensitivity as a function of phase shift. The optimum value of sensitivity is obtained at phase shift of 90°, which is in accordance with image rejection principle. Delay time as a function of sensitivity is also measured, as shown in Fig. 7(b). It is found that the best delay time is between 4 and 5 ps. In Fig. 7(c), the sensitivity keeps improving when the coupling factor is smaller than 0.5. The best sensitivity is obtained at coupling factor of 0.5 and then the sensitivity turns to deteriorate.

In conclusion, the detection method has limited the performance of the orthogonal FSK/ASK re-modulation in WDM-PON. We propose and demonstrate that adopting image rejection detection can efficiently overcome such a limitation. We compare the curves of image rejection detection and band-pass filter direct detection. The sensitivity is improved dramatically and the acceptable simulation result can also be obtained at 40 km. So the image rejection is suitable for super long reach optical access network. The image rejection is testified to be effective scheme to improve system performance when the FSK/ASK re-modulation is used and it will be promising in future PON.

This work was supported by the National "973" Project of China (No. 2010CB328300), the National Natural Science Foundation of China (No. 60777010), the National "863" Project of China (No. 2009AA01Z253), the Shuguang Found (No. 08SG05), the China Postdoctoral Science Foundation (No. 20090460593), and the Shanghai Postdoctoral Science Foundation (No. 10R21411600).

References

1. Q. Chang, J. Gao, Q. Li, and Y. Su, in *Proceedings of OFC 2008* OWH2 (2008).
2. B. Huang, X. Wang, Y. Liang, H. Liu, L. Wang, D. Huang, and N. Chi, in *Proceedings of ECOC 2008* Th.1.F.3 (2008).
3. G.-W. Lu, N. Deng, C.-K. Chan, and L.-K. Chen, in *Proceedings of OFC 2005* OFI8 (2005).
4. B. K. Kim, H. Park, S. Park, B. Y. Yoon, and B. T. Kim, in *Proceedings of ECOC 2006* (2006).
5. J. Zhang, X. Yuan, X. Ren, Y. Huang, and M. Zhang, in *Proceedings of SARNOFF 2009* 1–5 (2009).
6. C. H. Wang, F. Y. Shih, C. W. Chow, C. H. Yeh, and S. Chi, in *Proceedings of OFC 2009* JWA73 (2009).
7. W. Idler, A. Klekamp, R. Dischler, and B. Wedding, in *Proceedings of 2004 IEEE/LEOS Workshop Advanced Modulation Formats* 51 (2004).
8. X. Liu, Y. Shao, C. Hou, X. Zheng, X. Li, S. Zou, and N. Chi, in *Proceedings of ACP 2009* (2009).
9. Y. Shao, N. Chi, C. Hou, W. Fang, J. Zhang, B. Huang, X. Li, S. Zou, X. Liu, X. Zheng, N. Zhang, Y. Fang, J. Zhu, L. Tao, and D. Huang, J. Lightwave Technol. **28,** 1770 (2010).
10. T. Kawanishi, K. Higuma, T. Fujita, J. Ichikawa, T. Sakamoto, S. Shinada, and M. Izutsu, J. Lightwave Technol. **23,** 87 (2005).
11. K. Iwashita, Electron. Lett. **25,** 255 (1989).
12. B. F. Jørgensen, B. Mikkelsen, and C. J. Mahon, J. Lightwave Technol. **10,** 660 (1992).
13. T. Naitot, T. Chikama, S. Watanabe, and H. Kuwahara, Electron. Lett. **25,** 895 (1989).